DETERMINATION OF THE LARGEST STABLE SUDDENLY APPEARING AXIAL AND CIRCUMFERENTIAL THROUGH CRACKS IN DUCTILE PRESSURIZED PIPE

D. J. AYRES

Plant Engineering Department, Nuclear Power Systems, Combustion Engineering, Inc., 1000 Prospect Hill Road, Windsor, Connecticut 06095, U.S.A.

SUMMARY

The flow area from a postulated pipe break is an important parameter in the design of safety devices and the evaluation of safety margins for nuclear steam supply systems. Present design criteria assume that very long stationary cracks may exist, resulting in the prediction of large opening areas and fluid forces. A previous report by the author (3rd SMiRT Conference, Paper L7/6) presented the computations for the dynamic opening of two diameter long hypothetical axial cracks in nuclear system primary piping. These cracks are much longer than the maximum stable crack length and their opening therefore clearly provides a high upper bound to the fluid forces.

In this paper the largest stable cracks that could suddenly appear during normal operating conditions are determined by elastic-plastic dynamic finite element analysis. The stability of the hypothetical cracks is predicted by the J-integral ductile fracture criterion. The opening areas and the values of the J-integral for both axial and circumferential cracks are computed using the MARC-CDC general purpose finite element program.

Preliminary computations to verify the applicability of the thin shell finite element model were made with several thin shell models and a three dimensional solid model of a 21 inch (534 mm) long axial crack in a 42 inch (1068 mm) diameter 3.5 inch (89 mm) thick pipe. Elastic plastic dynamic analysis indicates that the suddenly appearing half diameter long axial crack is stable when subject to normal operating pressure. The crack opens to a maximum area of less than 2 in^2 (1290 mm^2) in 0.7 millisecond. A similar elastic plastic dynamic analysis was performed for a suddenly appearing three quarter diameter or 31.5 inch (800 mm) long axial crack under the same normal conditions. The J-integral computations indicate that this crack is not stable. The opening area computed for the three quarter diameter long crack reaches a maximum of less than 10 in^2 (6450 mm^2) in 1.7 milliseconds. These two cases indicate that the opening area of the largest stable axial crack in the 42 inch (1068 mm) diameter pipe is less than 10 in^2 (6450 mm^2).

In order to evaluate the stability and opening area of hypothetical circumferential cracks in 30 inch (762 mm) inside diameter 2.5 inch (63.5 mm) thick pipe is employed. The pipe is assumed to be under normal operating pressure and subject to the axial load caused by that pressure. A circumferential crack is assumed to suddenly appear with a length of half the circumference. The elastic plastic dynamic analysis results indicate that the crack is stable and reaches a maximum area of less than 6 in^2 (3870 mm^2) in 3.0 milliseconds. The computation indicates that a circumferential crack must exist more than half way around the circumference of the pipe before instability and a substantial crack opening area can occur.

The results of these analyses demonstrate that cracks in nuclear system primary piping must be greater than half diameter long for axial cracks, or half the circumference long for circumferential cracks before instability can occur during normal operation. These crack sizes, even when conservatively assumed to appear suddenly, open to areas which are very small fractions of the areas presently used in design.

1. Introduction

The flow area from a postulated pipe break is an important parameter in the design of safety devices and the evaluation of safety margins for nuclear steam supply systems. Present design criteria require the consideration of very long stationary axial cracks and total circumferential cracks. These hypothetical cracks result in the prediction of large opening areas and fluid forces. A previous report by Ayres [1] presented the results of dynamic opening analyses of two-diameter long hypothetical axial cracks in nuclear system primary piping. These cracks were shown to be much longer than the maximum stable crack length and their opening, therefore, clearly provides high upper bounds to the fluid forces.

In order to realistically determine the effects of suddenly appearing stable cracks, the largest stable axial and circumferential cracks must be determined.

Estimates of the largest stable cracks are made from linear elastic analysis. Detailed elastic plastic dynamic analyses are then performed using the estimated crack sizes in order to more precisely assess the stability in the ductile regime. All computations are performed on the MARC-CDC general purpose finite element program.

2. Preliminary Estimates

An analytical linear elastic analysis of axial cracks in cylinders was presented by Erdogan and Kibler [2]. For the 42-in. (1.07-m) inside diameter (ID) hot leg pipe, conservatively assumed to be 4 in. (0.1m) thick, at operating pressure, the static stress intensity factor for a 21-in. (0.53-m) long axial crack is 120 ksi $\sqrt{in.}$ (1.32×10^8 Pa $\sqrt{m}$) according to reference [2]. The static stress intensity factor for a 42-in. (1.07-m) long axial crack is 271 ksi $\sqrt{in.}$ (2.98×10^8 Pa $\sqrt{m}$). According to reference [1] the crack opening in the dynamic cases was about twice the opening in the corresponding static cases. If this ratio is applied to the stress intensity values, the dynamic stress intensities are 240 ksi $\sqrt{in.}$ (2.64×10^8 Pa $\sqrt{m}$) and 542 ksi $\sqrt{in.}$ (5.97×10^8 Pa $\sqrt{m}$) for the half-diameter and one-diameter long axial cracks.

Experimental burst studies on cracked pipes at Battelle, Eiber [3] have shown that ductile pipes have a maximum static toughness of around 250 ksi $\sqrt{in.}$ (2.75×10^8 Pa $\sqrt{m}$). Comparing this to the computed stress intensity factors suggests that the largest stable crack is nearly a half-diameter long in the 42-in. (1.07-m) diameter pipe.

3. Model Studies

The finite element analysis of reference [1] was adequate for the determination of the opening area of the crack. The computed stress intensity factor, however, was in the order of 16 percent below the accepted result of reference [2]. This magnitude of error at the crack tip is not acceptable for determination of critical crack length. The finite element model must be improved, therefore, for the subsequent detailed elastic plastic dynamic analysis to determine the critical crack length.

A schematic view of the pipe with an axial crack is shown in Figure 1. Since there are two planes of symmetry, only one quarter of the pipe is modeled. The boundary axially remote from the crack is permitted to move only axially and is loaded with the axial force caused by pressure. The finite element model of reference [1] is shown flattened out and not to scale in Figure 2. The static small displacement finite element analysis of half-diameter long axial crack in the 42-inch (1.07-m) ID pipe under 2250 psi (15.5×10^6 Pa) pressure results in a K_I of 85 ksi $\sqrt{in}$. (0.935×10^8 Pa $\sqrt{m}$) using the crack opening formula.

$$K_I = \frac{\delta E \sqrt{2\pi}}{4\sqrt{r}\,(1-\nu^2)} \qquad (1)$$

where δ is the crack opening at distance r from the crack tip and E and ν are Young's Modulus and poisson ratio respectively. In this case the displacement of the node closest to the crack tip, 0.05 a is used. The analytical solution according to reference [2] is 120 ksi $\sqrt{in}$. (1.32×10^8 Pa $\sqrt{m}$) indicating a substantial error for this crack size.

A finite element mesh similar to the shell model of reference [1] with a more refined grid near the crack tip is shown flattened out and not to scale in Figure 3. The finite element computation of K_I with this model and eq. (1), using the displacement at the closest node (0.01a), is 102 ksi $\sqrt{in}$. (1.12×10^8 Pa $\sqrt{m}$), and the K_I calculated from the next closest node (0.05a) is 128 ksi $\sqrt{in}$. (1.40×10^8 Pa $\sqrt{m}$).

Even with the refined mesh, the error in K_I computed from the closest node is substantial. This results from a poor representation of the elastic singularity close to the crack tip. K_I computed from the next point, the closest point in the original shell mesh, is in good agreement with the reference [2] solution. This indicates that the refined crack tip region describes more precisely the zone within 5 percent of the half-crack length away from the crack.

A finite element model of a half-diameter long crack in the hot leg made of twenty-noded three-dimensional elements is shown in Figure 4. This element has the capability of representing the elastic singularity at the crack tip (Barsoum [4]). The K_I calculated by elastic analysis for the point at the center of the wall using eq. (1) and the opening at the node closest to the crack tip (0.02a) is 117 ksi $\sqrt{in}$. (1.29×10^8 Pa $\sqrt{m}$).

This value is very close to the analytical result. The three-dimensional analysis is unacceptable for dynamic elastic plastic analysis, however, because the computer time is several times greater than the time for the shell analysis.

The refined shell mesh will be used because the resulting K_I values bracketed the analytical solution (and the three-dimensional analysis results). This indicates that the solution in the neighborhood of the crack is adequate and that a different technique for computing crack stability may be more appropriate. The J-integral, which integrates over the small crack tip region (Rice et. al [5]), is such a technique. The application of the J-integral as a fracture criterion will be discussed with the results of each analysis.

4. Analysis of a Half Diameter Long Axial Crack

An elastic plastic dynamic analysis of a half-diameter long axial crack in the 42-inch (1.07-m) ID pipe is performed with the refined shell model of Figure 3. The pipe is assumed to be operating at normal temperature and pressure when the crack suddenly appears. The analysis proceeds as described in reference [1].

An appropriate time step for the analysis can be chosen considering the lowest frequencies of the pipe. The lower frequencies of the pipe are computed to be about 165, 330, and 515 Hz. If a time step were chosen to be 0.01 milliseconds, and the stiffness damping factor β chosen to critically damp modes with periods less than four times the time step, then:

$$\beta = \frac{4\Delta T}{\pi} = 1.3 \times 10^{-5} \qquad (2)$$

This damping factor imposes less than 2 percent damping on modes with frequencies lower than 490 Hz. This damping then is acceptable for this analysis.

Using this time step and the damping factor just computed, the finite element model of Figure 3, and the procedure of reference [1], the opening of the crack is computed. Figure 5 shows the displacement of the point of maximum displacement (on the crack centerline) vs time. The maximum opening occurs at 0.72 milliseconds. The velocity of the same point during the opening is shown in Figure 6. The smoothness of the velocity demonstrates the stability of the solution. The crack opening shape is shown in Figure 7 along with elastic static results. The maximum opening area can be computed from Figure 7, by integrating under the plastic dynamic curve, to be 1.32 in^2 (851 mm^2). The crack opening shape is considerably different from those of reference [1]. In the case of the half-diameter crack, all the significant plasticity occurs near the crack tip. There is no significant bulging effect for a crack of this size. The half-diameter crack, therefore, can be considered a small crack (in spite of its 21-inch (0.53-m) axial length) since there is no significant interaction with the pipe geometry.

The stress, strain and displacement values computed by the finite element analysis are used to compute J from the definition

$$J = \int_\Gamma W.dy - T \frac{du}{dx} ds \qquad (3)$$

where x and y are rectangular coordinates normal to the crack front, ds is an increment of arc length along any contour, Γ, T is the stress vector on the contour, u is the displacement, and W is the strain energy density.

The results of J vs time during opening are shown in Figure 8. The J-integral increases smoothly until the maximum opening is reached. The peak in J-integral corresponds to the peak opening. The maximum value of J is 1467 in-lb/in^2 (25.8 J/cm^2).

The ductile fracture criterion states that crack extension occurs if J, during the event, becomes greater than J_{IC}, the critical value for the material at temperature. The criterion does not imply that if $J > J_{IC}$, the crack will become unstable. Prior to instability, some stable crack growth occurs. The amount of growth increases with increasing J. Research is presently being conducted (Wilkinson, et al [6]) to determine the extent of stable crack growth (the amount J can be increased above J_{IC}) before crack instability occurs.

The piping material, SA516 Gr 70 was tested for J_{IC} as a function of temperature using the precracked instrumented Charpy test in the Combustion Engineering Metallurgical and Materials Laboratory. Due to the nature of the test, J_{IC} values from instrumented charpy tests are probably somewhat greater than the real material parameter J_{IC}, since some stable crack extension is likely. A curve of J_{IC} vs temperature is shown in Figure 9. The data has the anticipated "S" shaped trend indicating the brittle to ductile transition in fracture. Also shown is the result of the opening computation. The computed J-integral is clearly below the critical value of J_{IC} indicating that the crack will not extend, and will remain stable. The difference is sufficiently large that small errors in computation or consideration of stable crack growth would not affect the conclusion concerning the stability of the crack.

5. Analysis of Three-Quarter Diameter Long Axial Crack

Since the half-diameter crack is stable, a longer crack will be assumed in order to determine the longest stable crack. It is desired to compute a conservative stable crack opening area so the assumed crack should be greater than the longest stable crack. These considerations led to the selection of a three-quarter diameter long crack as the next candidate for analysis. In order to compute a more conservative opening area, the minimum wall thickness of 3.5 in. (0.09 m) is used.

The time to open the three-quarter diameter long axial crack is greater than the time to open the half-diameter crack. If the same time step were used for this analysis, the computing cost would be substantially greater. Since the half-diameter long crack analysis was smooth with a time step of 0.01 milliseconds and the two-diameter long crack analyses were smooth with a time step of 0.1 milliseconds (reference [1]) a time step greater than 0.01 milliseconds will be attempted. A time step of 0.015 milliseconds was used at the beginning of the analysis. The associated stiffness damping factor according to eq. (2) is 1.91×10^{-5}. This damping factor imposes less than 2 percent damping on modes with frequencies lower than 335 Hz. This is acceptable since the first two modes are below this value.

As the analysis progressed, it became apparent from the smoothness of the solution, that the time step could be increased somewhat. After 0.54 milliseconds of opening the time step was increased to 0.02 milliseconds. The damping factor was unchanged. No numerical instability or irregularities were observed as a result of the time step change.

The opening displacement of the center of the three-quarter diameter long axial crack computed by the dynamic elastic plastic analysis is shown in Figure 10. The maximum opening occurs at 1.7 milliseconds. The velocity of the same point during the opening is shown in Figure 11. The smoothness of the curve illustrates the stability of the finite element solution. The maximum crack opening shape is shown in Figure 12. The maximum crack opening area computed from this opening shape is 9.6 in^2 (6210 mm^2). The J-integral computed during the opening is shown in Figure 13. These values were computed by the MARC program. The value in Figure 13 is the average value for two contour evaluations. One contour had a radius of 1 percent of the half-crack length and the other had a radius of 10 percent. The two evaluations never differed by more than 5 percent indicating an adequate level of path independence and a lack of inertia effects at the crack tip. The maximum J-integral value is 5500 in-lb/in^2 (96. J/cm^2), which is significantly greater than the measured value of J_{IC} in Figure 9.

Since the measured value of J_{IC} in Figure 9 is likely to be greater than the J for zero crack extension, and the computed J value is more than twice the measured one, it can be concluded that the computed J would cause significant crack extension. This crack extension would cause an increase in J which would lead to crack instability. The longest stable axial crack in the 42-inch (1.07-m) diameter pipe, then, can be concluded to be more than half but less than three-quarters of the diameter. The area computed for the three-quarter diameter long crack, then, is a conservative estimate for the opening area of the longest stable axial crack.

6. Analysis of a Half Circumference Crack

In order to evaluate the stability and opening area of hypothetical circumferential cracks, the 30-in. (0.76-m) ID, 2.5-in. (0.064-m) thick cold leg pipe is employed. The pipe is assumed to be under normal operating pressure of 2250 psi (15.5×10^6 Pa) and subject to the axial load caused by that pressure. A circumferential crack is assumed to suddenly appear with a length of half the circumference of the pipe. A schematic view of the pipe containing the circumferential crack is shown in Figure 14. Since two planes of symmetry exist, one quarter of the pipe can be modeled. The finite element model of one-quarter of the pipe is shown flattened out and not to scale in Figure 15. The boundary axially remote from the crack is permitted to move axially and rotate as a plane. The force on the boundary is the axial force caused by the pressure. As in the case of the axial cracks, no depressurization due to the crack opening is assumed.

The lower frequencies of the finite element model of the cold leg pipe were computed to be 76 Hz, 207 Hz, and 275 Hz. The time step of 0.015 milliseconds was used for the beginning of the analysis. The damping factor of 1.91×10^{-5} was also used. After 0.45 milliseconds of opening, the time step was increased to 0.02 milliseconds. The time step was gradually increased to 0.1 milliseconds by 1.65 milliseconds into the opening analysis. Again, no numerical instabilities or irregularities occurred as a result of increasing the time step during the analysis.

The opening displacement of the center of the crack computed by the dynamic elastic plastic analysis is shown in Figure 16. The maximum opening occurs at 3.0 milliseconds. The velocity of the same point is shown in Figure 17. The vibration of the pipe as a beam is clearly seen in this Figure. The smoothness of the velocity curve demonstrates the numerical stability of the solution. The maximum opening shape is shown in Figure 18. The crack opening area during the opening is shown in Figure 19. The maximum value is 5.3 in.^{2} (3420 mm^2).

The J-integral computed during the opening is shown in Figure 20. These values were computed by MARC and are the average of two near crack contours. The maximum J-integral value is 1250 in-lb/in^2 (21.8 J/cm^2) which is significantly below the J_{IC} curve of Figure 9. It can be concluded in this case, then, that the circumferential crack, halfway around the pipe, will not be unstable if it suddenly appears during normal operating conditions. In order for a crack to become a full circumference crack it must suddenly appear greater than halfway around the circumference.

7. Conclusions

The results of these analyses demonstrate that cracks in nuclear steam supply system primary piping must occur between one-half diameter and three-quarters diameter in length for axial cracks or between half circumference and full circumference in length for circumferential cracks before instability can occur during normal operation. The largest stable crack sizes, even when conservatively assumed to appear suddenly, open to areas that are very small fractions of the areas presently used in design.

References

[1] AYRES, D. J., "Elastic Plastic Dynamic Analysis of Opening Area of an Axial Crack in a Pipe Under Pressure," Paper L 7/6, 3rd International Conference on Structural Mechanics in Reactor Technology, London, U.K., September, 1975.

[2] ERDOGAN, F., and KIBLER, J. J., "Cylindrical and Spherical Shells with Cracks," Int. Journal of Fracture Mechanics 5(1969) pp. 229-237.

[3] EIBER, R. J. et al, "Investigation of the Initiation and Extent of Ductile Pipe Rupture," Battelle Memorial Institute (BMI-1866) July 1969.

[4] BARSOUM, R. S., "Application of Quadratic Isoparametric Finite Element in Linear Fracture Mechanics," Int. Journal of Fracture (Reports of Current Research) December 1974.

[5] RICE, J. R., PARIS, P. C., and MERKLE, J. G., "Some Further Results of J-Integral Analysis and Estimates," Progress in Flaw Growth and Fracture Toughness Testing, STP536, ASTM 1973.

[6] WILKINSON, G. P. D., et al, "Methodology for Plastic Fracture," First Quarter Report #SRD-76-100, Prepared by General Electric Co. for the Electric Power Research Institute, September 10, 1976.

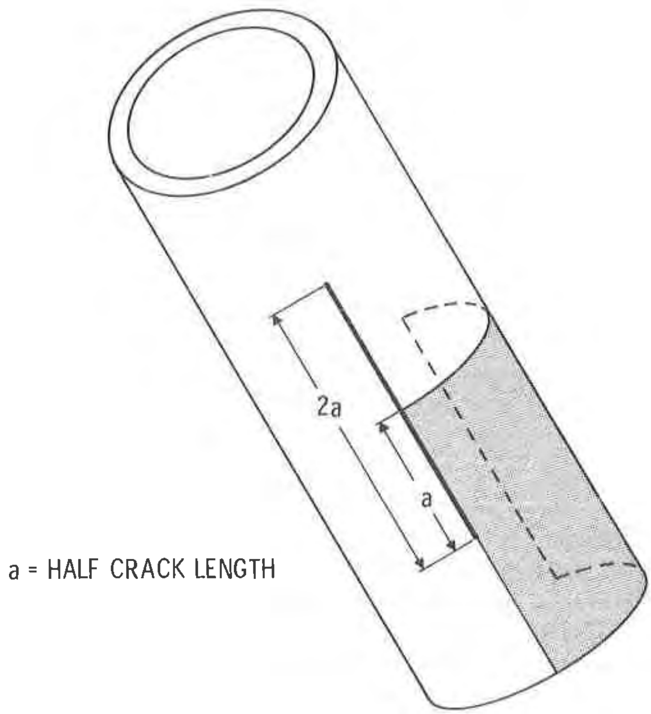

Fig. 1: Geometry of pipe with hypothetical axial crack

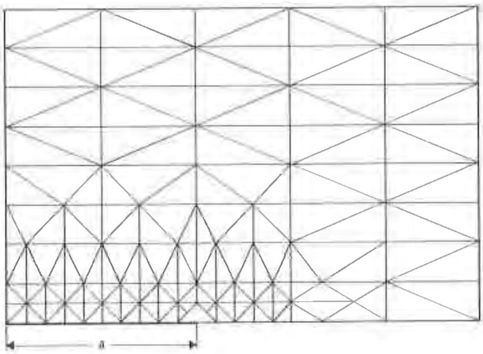

Fig. 2a: Shell model of reference 1 crack tip region

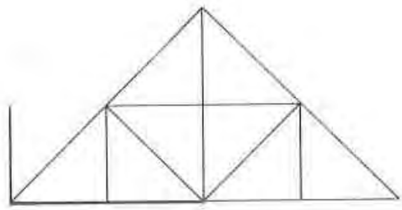

Fig. 2b: Shell model of reference 1 remote from crack tip

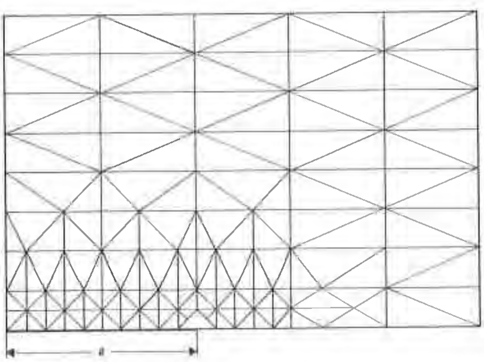

Fig. 3a: Refined shell model remote from crack tip

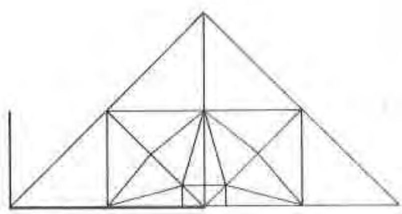

Fig. 3b: Refined shell model crack tip region

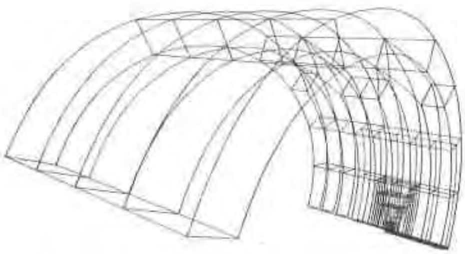

Fig. 4: Half-diameter long axial crack three-dimensional model

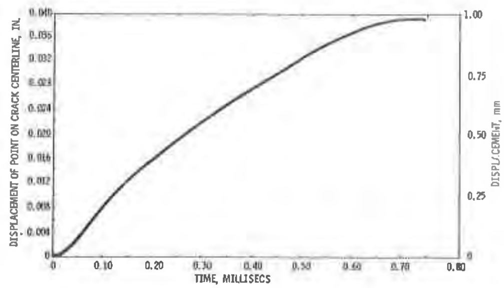

Fig. 5: Displacement of point on crack centerline - half-diameter long axial crack

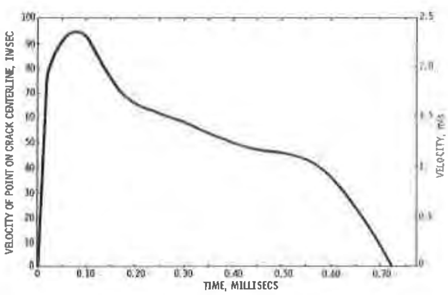

Fig. 6: Velocity of point on crack centerline vs. time during opening half-diameter long axial crack

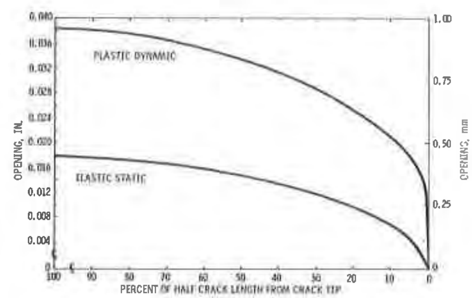

Fig. 7: Half-diameter long axial crack opening shape at maximum opening

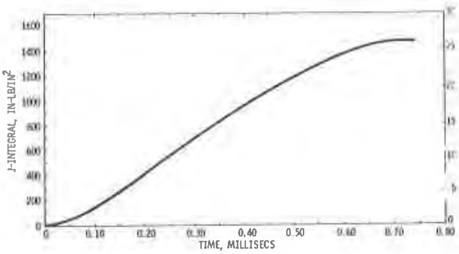

Fig. 8: J-integral vs. time during opening of half-diameter long axial crack

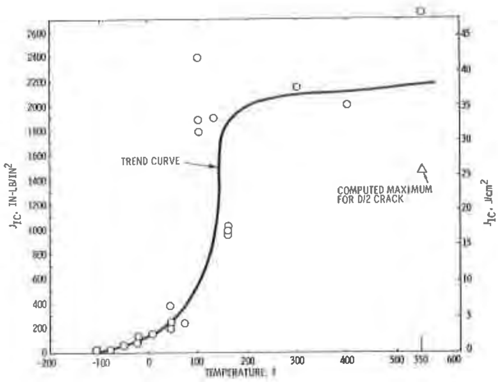

Fig. 9: J-integral (J_{IC}) vs. temperature for SA 516 GR 70

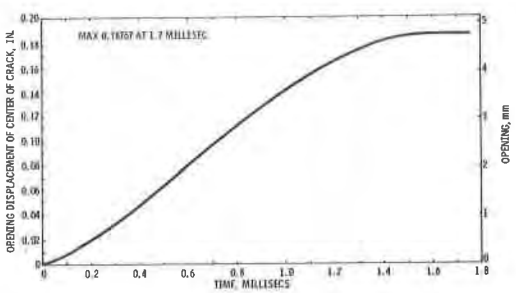

Fig. 10: Displacement of point on crack centerline three-quarter diameter long axial crack

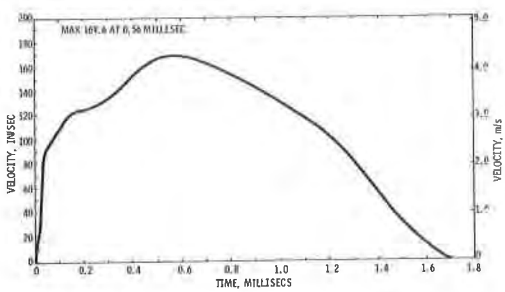

Fig. 11: Velocity of point on crack centerline vs. time during opening three-quarter diameter long axial crack

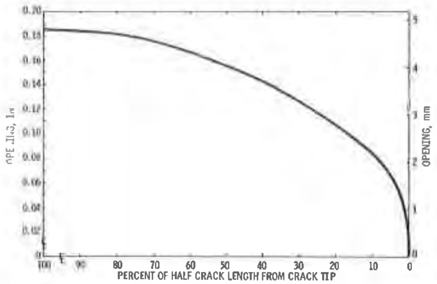

Fig. 12: Three-quarter diameter long axial crack opening shape at maximum opening

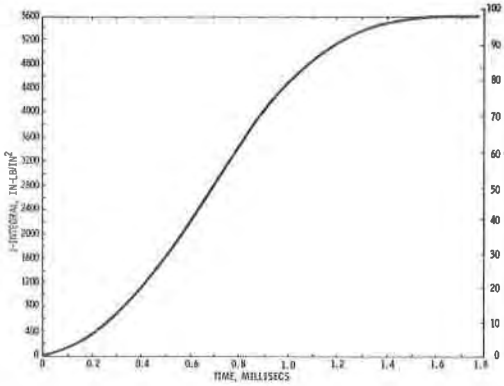

Fig. 13: J-integral vs. time during opening of three-quarter diameter long axial crack

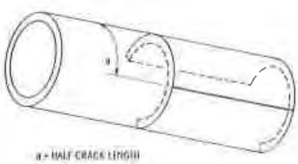

Fig. 14: Geometry of pipe with hypothetical half-circumference crack

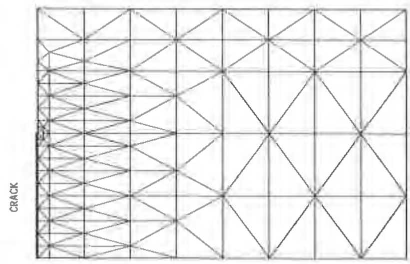

Fig. 15: Shell model for half-circumference crack in pipe

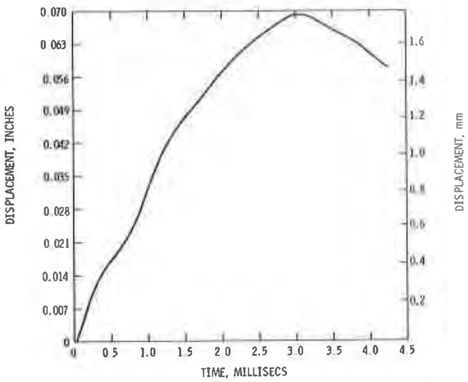

Fig. 16: Displacement of point on crack centerline - half-circumference crack

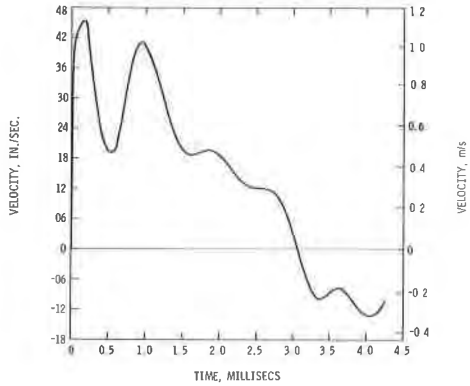

Fig. 17: Velocity of point on crack centerline vs. time during opening half-circumference cra

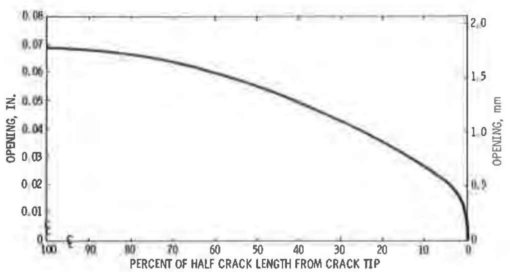

Fig. 18: Half-circumference crack opening shape at maximum opening

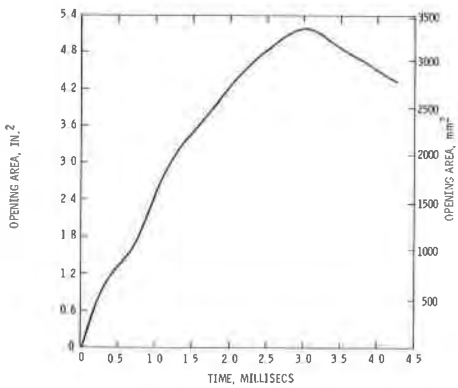

Fig. 19: Opening area of half-circumference crack vs. time

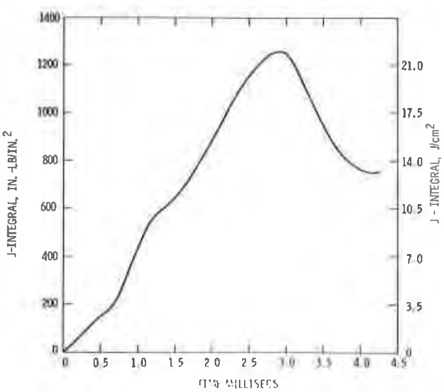

Fig. 20: J-integral vs. time during opening of half-circumference crack